

# Removal of fluoride from drinking water using aluminum hydroxide coated activated carbon prepared from bark of *Morinda tinctoria*

Augustine Amalraj<sup>1</sup> · Anitha Pius<sup>1</sup>

Received: 24 August 2015 / Accepted: 26 September 2016 / Published online: 12 October 2016  
© The Author(s) 2016. This article is published with open access at Springerlink.com

**Abstract** The aim of this study is to design and develop a novel cost effective method for fluoride removal, applicable to rural areas of developing countries. Adsorption is widely considered as one of the appropriate technologies for water defluoridation. This study investigates the feasibility of using low-cost biomass based activated carbon from the bark of *Morinda tinctoria* coated with aluminum hydroxide (AHAC) for water defluoridation, at neutral pH range. Characterization of AHAC was done through IR, SEM with EDAX studies before and after fluoride treatment. The fluoride adsorption capacity of AHAC as a function of contact time, pH and initial fluoride concentration was investigated. The role of co-existing interfering ions also was studied. The isotherm and kinetic models were used to understand the nature of the fluoride adsorption onto AHAC. Freundlich isotherm and intra-particle diffusion were the best-fitting models for the adsorption of fluoride on AHAC. Fluoride adsorption kinetics well fitted with pseudo-second order model. The results showed excellent fluoride adsorption capacity was found to be 26.03 mg g<sup>-1</sup> at neutral pH.

**Keywords** Aluminum hydroxide coated activated carbon · Fluoride removal · *Morinda tinctoria* · Adsorption isotherm · Adsorption kinetics

## Introduction

The quality of drinking water is very important for public health and for better life. Optimum concentration of fluoride (about 1 mg L<sup>-1</sup>) in drinking water is good for dental health and for good bone development. Intake of excess fluoride (beyond 1.5 mg L<sup>-1</sup>, WHO guideline) (WHO 2006) for long periods can result in the incidence of fluorosis. Low concentrations of fluoride in drinking water have been considered beneficial to prevent dental carries. But researchers are now debating on the health benefits of fluoride even at low concentrations. It has long been known that chronic intake of fluoride even though below 1 mg L<sup>-1</sup> can lead to severe dental and skeletal fluorosis. It not only affects teeth and skeleton, but its accumulation over a long period can also lead to loss of mobility, lowering of IQ of children, change in the DNA structure and interference with liver and kidney functioning (Chen et al. 2011; WHO 2008; Xiong et al. 2007).

Endemic fluorosis is prevalent in at least 25 countries across the globe including India, Argentina, China, Tanzania, Serbia and Srilanka (Ayoob and Gupta 2006; Das et al. 2005; Kruse and Ainchil 2003; Ba et al. 2009; Shorter et al. 2010; Mandinic et al. 2010; Waidyasekera et al. 2007) and more than 200 million people worldwide are affected by excess concentration of fluoride, in their drinking water (Mohan et al. 2012). In India, there has been an increase in the incidence of dental and skeletal fluorosis with about 62 million people at risk (Das et al. 2005). High concentrations of fluoride in groundwater are common in all the states of India particularly Andhra Pradesh, Haryana, Karnataka, Maharashtra, Rajasthan, Tamil Nadu and West Bengal (Ayoob and Gupta 2006; Meenakshi and Maheshwari 2006; Amalraj and Pius 2013).

✉ Anitha Pius  
dranithapius@gmail.com

<sup>1</sup> Department of Chemistry, The Gandhigram Rural Institute-Deemed University, Gandhigram, Dindigul, Tamil Nadu 624 302, India

In India, the fluoride content in ground water tends to increase due to heavy withdrawal of water for agriculture purpose, poor recharging, low rainfalls and pollution from industrial effluents. Some reports evidenced that the adverse health effects of fluoride are enhanced by lack of calcium, vitamins, and protein in the diet (Li et al. 1996; Jacks et al. 1993). India has declared fluorosis as an epidemic and has banned the use of water for drinking and cooking if the fluoride content is more than  $1.5 \text{ mg L}^{-1}$ . According to World Health Organization guidelines, the fluoride concentration in drinking water should not exceed  $1.5 \text{ mg L}^{-1}$  (WHO 2006). However, this guideline value of fluoride is not universal. Latest guidelines from the Bureau of Indian Standards (BIS) suggest (Susheela and Majumdar 1998) that the fluoride limit in ground water used for drinking and cooking purposes should not be greater than  $1 \text{ mg L}^{-1}$ . Defluoridation of drinking water is thus important to safeguard public health.

Nowadays, several techniques have been developed for treating fluoride-polluted water. The commonly used methods for fluoride removal include coagulation, separation, precipitation, adsorption, ion-exchange, electrolysis, electro dialysis, electrochemical methods and reverse osmosis (Meenakshi and Maheshwari 2006; Fawell et al. 2006; Vasudevan et al. 2009, 2011, 2014). In comparison to the above mentioned techniques for fluoride removal from drinking water, adsorption process is widely considered the most appropriate defluoridation technique. This is due to its flexibility and simplicity of design, relative ease of operation, cost effectiveness and it produces high-quality of water (Lesmana et al. 2009; Kumar et al. 2009). The search for alternative and suitable fluoride adsorbents therefore still remains of interest.

Activated carbon (AC) is considered as the universal adsorbent for removing pollutants from water due to its high porosity, large surface area, and versatile surface chemistry (Hernandez-Montoya et al. 2012). Since the operational costs of adsorption are mainly determined by the price of the adsorbent, there is a growing interest in looking for alternative precursors in AC production. The interest is growing in fluoride removal by biomass based chemically modified activated carbon due to their lower cost and availability. The chemically modified bio-sorbents such as calcium pretreated algal biomass (Bhatnagar et al. 2002), aluminum hydroxide coated rice husk (Ganvir and Das 2011), cashew nut shell (Alagumuthu and Rajan 2010), zirconium impregnated coconut shell (Sathish et al. 2007) and tamarind fruit shell carbon (Sivasankar et al. 2012) are reported as fluoride scavengers in water. However, there are very little studies on the use of activated carbon prepared from biomass particularly wood and bark of trees (Salame and Bandosz 2000), whereas selected bark is

largely available, inexpensive and may lead to preparation of activated carbons.

The aim of the present work is to prepare activated carbon by carbonization of bark of *Morinda tinctoria* using sulfuric acid and to modify the surfaces of activated carbon with aluminum hydroxide coating for fluoride adsorption. In this study fluoride adsorption is based on the application of the hard and soft acids and bases (HSAB) concept, and also on exploring the suitability of using locally available materials. Due to its high electronegativity and small ionic size, the fluoride ion is classified as a hard base, which has a strong affinity towards  $\text{Al}^{3+}$  which is classified as a hard acid, therefore  $\text{Al}^{3+}$  has good affinity towards  $\text{F}^{-}$  ion.

The fluoride adsorption potential of the aluminum hydroxide coated activated carbon (AHAC) has been investigated in batch system. The physicochemical characteristics of AHAC were examined with SEM, EDAX and FT-IR studies. The impact of thermal treatment of AHAC on its fluoride adsorption capacity was also investigated. The effects of contact time, pH and initial concentration on fluoride removal by AHAC were also examined.

## Materials and Methods

### Chemicals

All chemical reagents used in this work were of analytical grade (AR). Aluminum sulfate [ $\text{Al}_2(\text{SO}_4)_3 \cdot 16\text{H}_2\text{O}$ ], sulfuric acid ( $\text{H}_2\text{SO}_4$ ), sodium hydroxide (NaOH), sodium nitrate ( $\text{NaNO}_3$ ), sodium sulfate ( $\text{Na}_2\text{SO}_4$ ), sodium bicarbonate ( $\text{NaHCO}_3$ ), sodium chloride (NaCl) and sodium fluoride (NaF) were purchased from Sigma-Aldrich, India. Milli-Q ultra pure water was used throughout the study.

### Preparation of activated carbon by chemical activation

Bark of *M. tinctoria* collected locally were used in this study. The collected barks were cut into small pieces and were dried in an oven at  $105 \text{ }^\circ\text{C}$  to constant weight and then immersed in concentrated sulfuric acid for 4 h. The impregnated bark was dried at  $160 \text{ }^\circ\text{C}$  till complete charring for another 4 h. The char was then washed with Milli-Q ultra pure water until it was free from acid (Amalraj and Pius 2014). The activation was completed by heating for 12 h in a furnace at  $400 \text{ }^\circ\text{C}$  to enhance the porous nature of the activated carbon. The resulting AC was washed with Milli-Q ultra pure water and dried for 4 h at  $100 \text{ }^\circ\text{C}$  in a hot air oven. The dried adsorbent was ground and stored in separate vacuum desiccators for further studies.

## Synthesis of aluminum hydroxide coated activated carbon (AHAC)

Synthesis of AHAC was carried out with suitable modification explained by (Ganvir and Das 2011). Five hundred milliliter of 0.6 M aluminum sulfate solution was taken in a reactor tank with stirrer, which was followed by slow addition of 100 g of already prepared AC to the reactor tank with proper mixing to ensure complete soaking of AC in aluminum sulfate solution. Then, 3 M sodium hydroxide solution was slowly added to the reactor while stirring at 200 rpm. Sodium hydroxide reacts with aluminum sulfate to produce precipitate of aluminum hydroxide, which gets deposited on AC surface. The addition of the sodium hydroxide was stopped when the pH reaches 7. The resultant slurry mixture contained aluminum hydroxide (AH) coated AC and sodium salt. This was filtered using vacuum to produce a filter cake of AHAC and it was dried in the oven at 110 °C at 5 h. The AHAC was washed thoroughly with Milli-Q ultra pure water to remove sodium sulfate salt. The washing was done till the output water shows less than 1 mg L<sup>-1</sup> of sulfate ions. Then washed AHAC was again dried in an oven at 100 °C for 5 h. This washed and dried AHAC was characterized and used for the batch adsorption studies for the fluoride removal.

## Adsorption experiments

Fluoride stock solution of 1000 mg L<sup>-1</sup> was prepared by dissolving 2.21 g of anhydrous NaF in one litre of distilled water. Test solution of 10 mg L<sup>-1</sup> fluoride concentration was prepared from the stock solution. All the experiments were carried out in 250 mL conical flasks with 0.1 g of adsorbent and 100 mL of test solution. The contents were shaken thoroughly using a thermostated shaker rotating at a speed of 200 rpm to study various parameters. At the end of desired contact time, the conical flasks were removed and filtered using Whatman No. 1 filter paper. Fluoride levels in filtrate were measured by using fluoride ion selective electrode Orion ion analyzer (Thermo scientific Orion 4 Star) by diluting with total ionic strength adjustment buffer (TISAB III) in 10:1 ratio. The instrument was calibrated with standard fluoride solutions so chosen that the concentration of one was ten times the concentration of the other and also that the concentration of the unknown falls between those standards. Then the concentration of the unknown was directly read from the digital display of the meter (Orion Star and Star Plus Meter User Guide 2008). Batch study was conducted to determine the optimum conditions. The effects of pH, adsorbent dose, initial fluoride concentration, and contact time on adsorption were investigated. The effect of pH on fluoride was studied by adjusting the pH of test solution using 0.1 M HCl or 0.1 M NaOH on fixed quantity of adsorbent. For the temperature studies, the effect of different initial

fluoride concentrations viz., 2, 6 and 10 mg L<sup>-1</sup> at 303, 313 and 323 K on adsorption rate was studied by keeping the mass of sorbent as 0.1 g and volume of solution as 100 mL at neutral pH. The solution was then filtered and the residual fluoride ion concentration was measured. Duplicate experiments were performed in parallel to get concordant results. The results showed that the error was within 2 %.

## Co-ion interference studies

The influence of co-existing ions on the adsorption capacity of AHAC was investigated for fluoride concentration of 10 mg L<sup>-1</sup> at neutral pH with equilibrium time of 60 min. Various co-ion solutions of 50 mg L<sup>-1</sup> prepared for the study were NaNO<sub>3</sub>, Na<sub>2</sub>SO<sub>4</sub>, NaHCO<sub>3</sub>, and NaCl based on the presence of these ions in the field sample analysis.

## Applications to groundwater samples

Defluoridation of groundwater samples contain more than 3 mg L<sup>-1</sup> fluoride was explored for samples from various locations of Nilakottai block in Dindigul District. The physicochemical parameters for the ground water samples were also determined in accordance with standard procedure of the American Public Health Association (APHA) before and after adsorption experiments (APHA 2005).

## Results and discussion

### Characterization of AHAC

The FT-IR spectra have shown in Fig. 1a, b represent the AHAC and fluoride-adsorbed AHAC. The broad band at

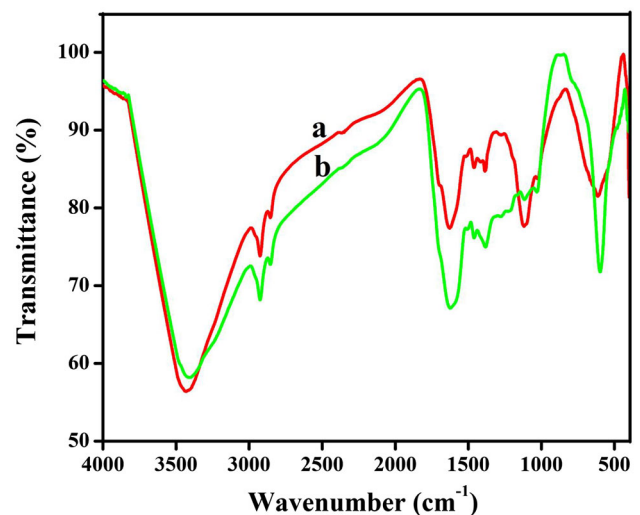


Fig. 1 FTIR spectra of a AHAC and b fluoride adsorbed AHAC

3430  $\text{cm}^{-1}$  was ascribed to the stretching vibration of hydroxyl functional groups including hydrogen bonding. The band at 2925  $\text{cm}^{-1}$  indicates the  $-\text{CH}$  stretching vibration in  $-\text{CH}$  and  $-\text{CH}_2$ . The peak at 2854  $\text{cm}^{-1}$  indicates the presence of aliphatic  $\text{C}-\text{H}$  stretching. The presence of aromatic groups in the AHAC is evidenced by the peak at 1629  $\text{cm}^{-1}$  may be related to aromatic  $\text{C}-\text{C}$  vibration (Amalraj and Pius 2014; Lua and Yang 2004; Khaled et al. 2009). The bands at around 1461 and 1387  $\text{cm}^{-1}$  correspond to  $\text{C}-\text{H}$  in plane bending vibrations in methyl and methylene groups, respectively (Yang and Qiu 2010). The sharp peak at 1118  $\text{cm}^{-1}$  could be due to  $\text{C}-\text{O}$  stretching vibration (Ma et al. 2009). The bands observed at 1027  $\text{cm}^{-1}$  could be from vibrations of aluminum oxide. In addition the metal–oxygen stretching mode was observed at 615  $\text{cm}^{-1}$  (Das et al. 2003; Legrouiri et al. 1999). After fluoride adsorption, a broadening of band at 3407  $\text{cm}^{-1}$  in the fluoride adsorbed AHAC may be taken as an indication of electrostatic adsorption between the adsorbent and the fluoride (Viswanathan and Meenakshi 2009) and also the band observed at 598  $\text{cm}^{-1}$  is very strong, sharp and symmetric. This could be due to the reconstruction of the metal oxide in the presence of fluoride (Das et al. 2003) onto AHAC.

SEM pictures of AHAC and the fluoride-adsorbed AHAC are shown in Fig. 2a, b, respectively. The change in the SEM micrographs of the AHAC before and after fluoride treatment indicates structural changes in the

adsorbent. This is additionally supported by EDAX analysis which provides the direct proof for the adsorption of fluoride ions onto AHAC. The EDAX spectra of AHAC and the fluoride adsorbed AHAC confirm the presence of respective ions in the Fig. 3a, b. The fluoride adsorption has occurred on AHAC which was confirmed by the presence of aluminum and fluoride peaks in the EDAX spectra of fluoride treated AHAC.

### Effect of contact time

The fluoride adsorption capacity of AHAC was determined by varying the contact time in the range of 10–100 min at 0.1 g dose and with 10  $\text{mg L}^{-1}$  initial fluoride concentration in neutral pH at 303 K. As shown in Fig. 4, the adsorbent AHAC reached saturation at 60 min. and thereafter remains almost constant. The adsorption reaction was faster initially due to the participation of particular functional groups and active surface sites on adsorbent's surfaces. Presence of such surfaces and functional groups on chemically modified AC was reported earlier by other researchers as well (Ganvir and Das 2011; Salifu et al. 2013). Furthermore, the analysis was carried out to estimate the presence of any traces of aluminum after treated water by atomic absorption spectrometer (Perkin–Elmer A Analyst 100). Instrumental conditions: wavelength = 309.3 nm, slit = 0.7 nm, recommended flame =  $\text{N}_2\text{O}$ –acetylene (rich, red) and nebulizer = spoiler. Calibration

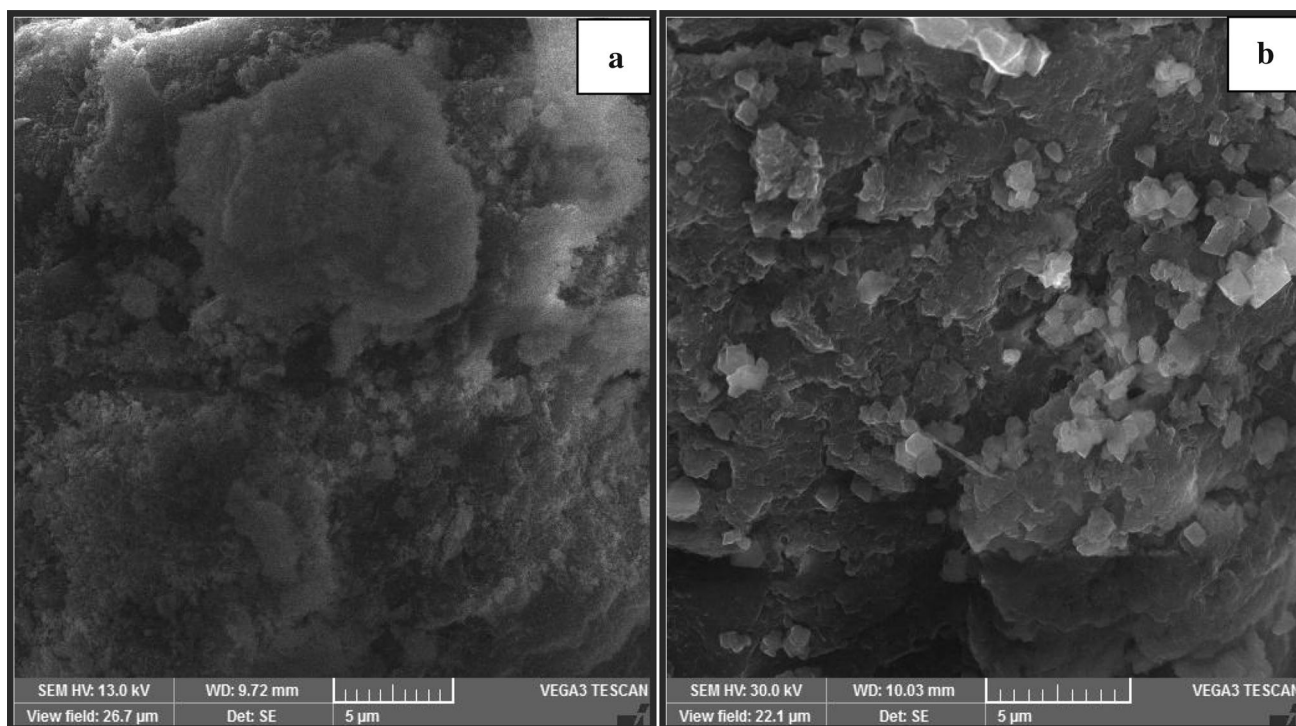
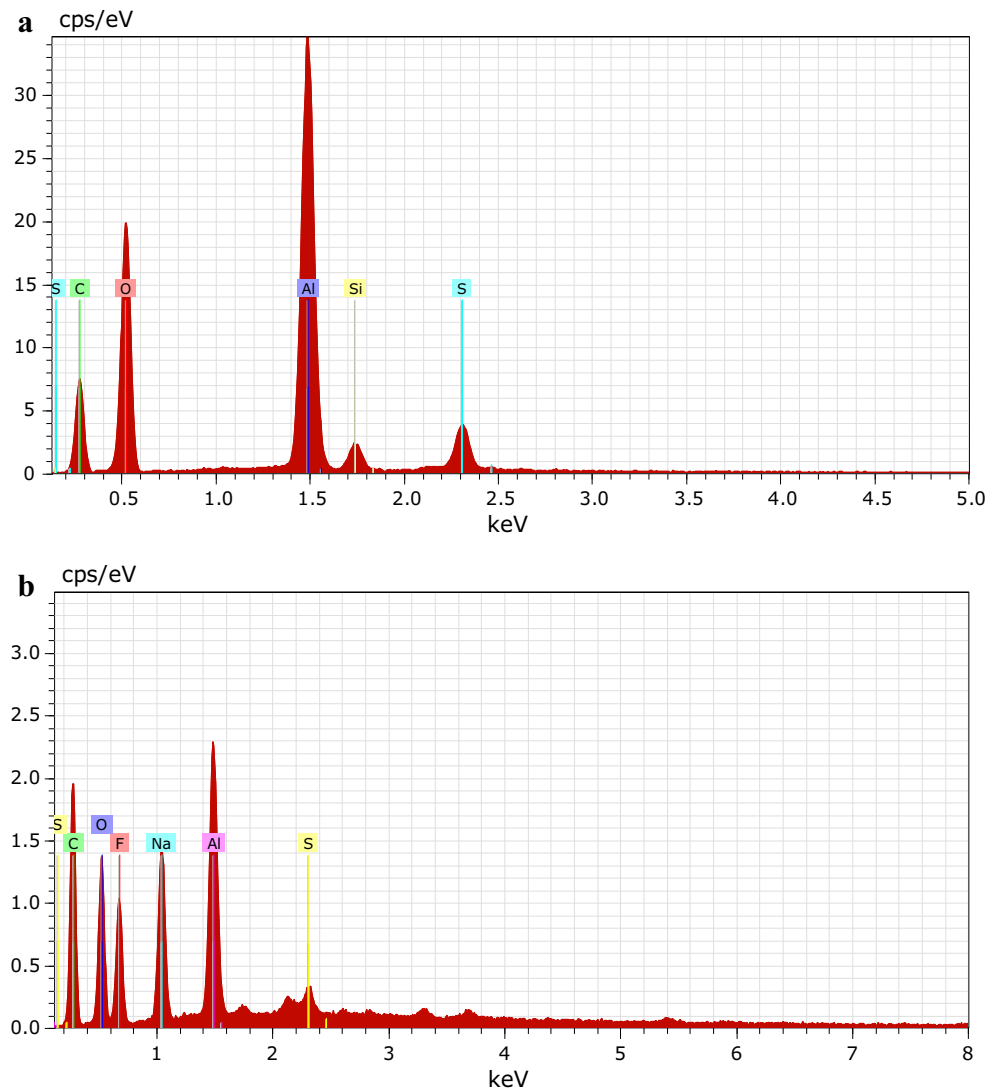


**Fig. 2** SEM images of **a** AHAC and **b** fluoride adsorbed AHAC

**Fig. 3** EDAX spectra of **a** AHAC and **b** fluoride adsorbed AHAC



of the instrument was performed using commercial standards. All measurements were carried out using standard flame operating conditions, as recommended by the manufacturer. The results showed that there were no traces of aluminum after treated water. It is clearly indicated that the aluminum hydroxide well coated with activated carbon.

### Effect of pH

In most of the solid/liquid adsorption processes, the solution pH has great importance in deciding the adsorption potential of the adsorbent, because it alters the surface charge on the adsorbents (Meenakshi et al. 1991; Kamaraj et al. 2015a, b). Hence the fluoride uptake capacity onto the AHAC was studied at seven different initial pH levels viz., 1, 3, 5, 7, 9, 11 and 13 by keeping 60 min as contact time, 0.1 g adsorbent dose and  $10 \text{ mg L}^{-1}$  as initial fluoride concentration at 303 K. The pH of the working solution

was controlled by adding HCl/NaOH solutions. Figure 5 shows the fluoride removal capacity of the AHAC as a function of pH and the maximum fluoride removal took place at neutral pH. In the acidic pH range, the amount of fluoride adsorbed is decreased and this can be attributed to the formation of weak hydrofluoric acid and may also be attributed to the complexation of fluoride ions with aluminum (Raichur and Basu 2001). Beyond neutral pH, a progressive decrease in fluoride removal was observed. This may be mainly attributed to the competition for the active sites by  $\text{OH}^-$  ion and the electrostatic repulsion of fluoride ions by the negatively charged AHAC surface (Maliyekkal et al. 2008).

### Effect of initial fluoride concentration

The effect of initial fluoride concentration was investigated by adding fixed amounts of adsorbents onto solutions with

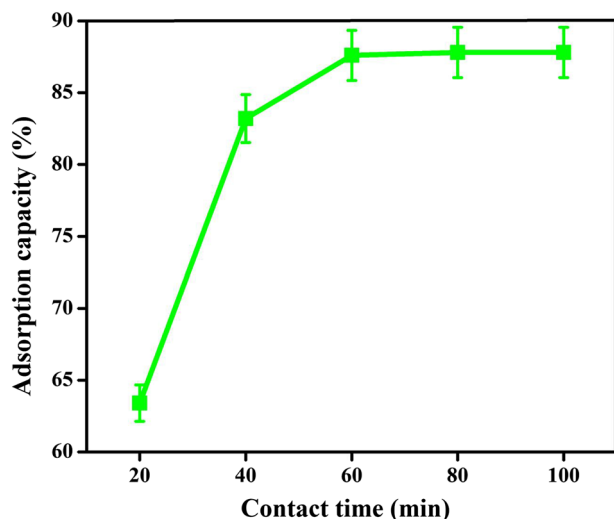


**Fig. 4** Effect of contact time on fluoride removal (0.1 g of adsorbent in 100 mL of a solution at  $10.0 \text{ mg L}^{-1}$ )

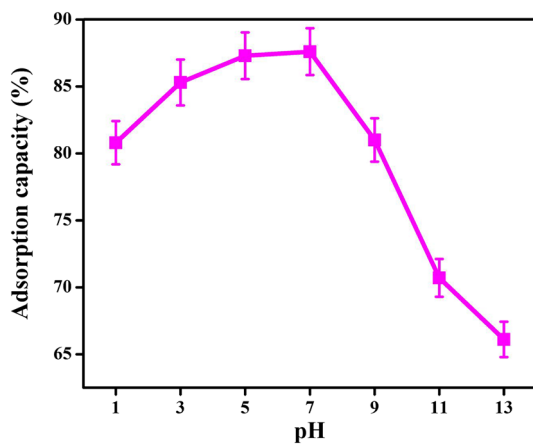


**Fig. 5** Effect of pH on fluoride removal (0.1 g of adsorbent in 100 mL of a solution at  $10.0 \text{ mg L}^{-1}$ )

different fluoride concentrations viz., 2, 4, 6, 8 and  $10 \text{ mg L}^{-1}$ . The effect of initial fluoride concentration on the fluoride adsorption capacity is illustrated in Fig. 6. The results illustrated that fluoride adsorption capacity was decreased, by increasing the initial fluoride concentration. The reason is that the capacity of the adsorbent materials gets exhausted sharply with the increase in initial fluoride concentration. This is due to the fact that for a fixed adsorbent dose, the total available adsorption sites were limited, which became saturated at a higher concentration.

#### Effect of co-existing ions

The contaminated ground water contains several other coexisting ions also along with fluoride, which may compete with fluoride for the active adsorption sites. Hence, it is important to investigate the interference of co-existing

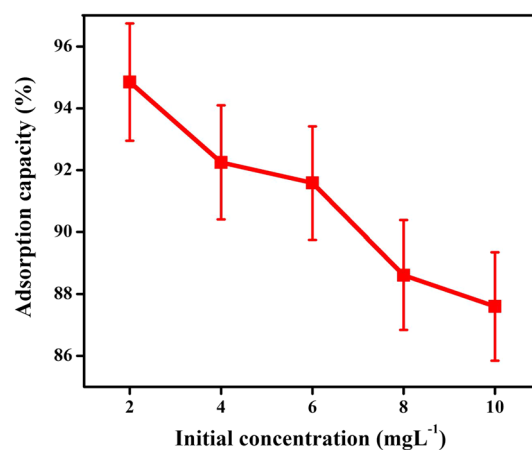


**Fig. 6** Effect of initial concentration on fluoride removal (0.1 g of adsorbent in 100 mL of a solution)

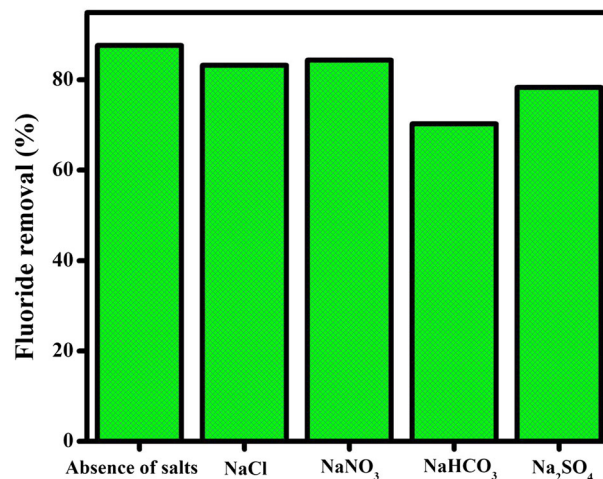


**Fig. 7** Effect of co-anions on the fluoride removal (0.1 g of adsorbent in 100 mL of a solution at  $10.0 \text{ mg L}^{-1}$  of fluoride and  $50.0 \text{ mg L}^{-1}$  of other co-anions)

ions on fluoride adsorption onto AHAC for evaluating the suitability of AHAC for field applications. The influence of coexisting ions bicarbonate, sulfate, chloride and nitrate on fluoride adsorption was studied and shown in Fig. 7. The presence of mono-valent ions except  $\text{HCO}_3^-$  that is  $\text{NO}_3^-$  and  $\text{Cl}^-$  showed little effect on fluoride adsorption because of the formation of weak bonds with the active sites at the outer-sphere complex. The leading competitor against fluoride is bicarbonate, which is the conjugate base of a weak acid, produces hydroxyl ions. These resulting hydroxyl ions compete against fluoride for the same sites (Sivasankar et al. 2012; Onyango et al. 2004). The divalent nature of sulfate ion in solution may influence strong coulombic repulsive forces which lead to lessen fluoride interaction with the active sites (Eskandarpour et al. 2008). The decrease in the fluoride uptake (Fig. 7) may be due to the competition between fluoride and other ions for the

active sites on the surface of AHAC. From the results, it may be inferred that the fluoride adsorption capacity on AHAC may be altered by the presence of other competing ions.

### Adsorption isotherms

To quantify the adsorption capacity of AHAC for the removal of fluoride, three isotherms namely Freundlich (Freundlich 1906), Langmuir (Langmuir 1916) and Dubinin–Radushkevich (D–R) (Bering et al. 1972) have been adopted. The linear forms of Freundlich, Langmuir and Dubinin–Radushkevich are given in Table 1.

#### Freundlich isotherm

The Freundlich model is an empirical equation based on adsorption on a heterogeneous surface. The linear form of Freundlich isotherm (Freundlich 1906) is given in Table 1. The Freundlich isotherm constants  $1/n$  and  $k_F$  were calculated from the slope and the intercept of the plot of  $\log q_e$  vs  $\log C_e$ . These constants related to the measure of adsorption intensity or surface heterogeneity and adsorption capacity, respectively and the constant values are given in Table 2. Values of  $1/n$  lying between 0 and 1 and the  $n$ -values lying in the range of 1–10 confirm the favorable conditions for adsorption (Sivasankar et al. 2012). The adsorption capacity  $k_F$  increases with increase in temperature suggesting that the fluoride adsorption on AHAC is an endothermic process.

#### Langmuir isotherm

The fluoride adsorption capacity of AHAC has been evaluated using Langmuir isotherm model (Langmuir 1916). The linear plot of  $C_e/q_e$  vs.  $C_e$  indicates the applicability of Langmuir isotherm on the fluoride adsorption capacity of AHAC. The values of Langmuir constants are given in Table 2. The Langmuir constants  $Q^0$  and  $b$  are related to adsorption capacity and adsorption energy, respectively. Maximum adsorption capacity ( $Q^0$ ) represents monolayer coverage of sorbent with sorbate and  $b$  represents the energy of adsorption and varies with temperature.

To find out the probability of isotherm, the important characteristics of Langmuir isotherm can be expressed in

terms of a dimensionless constant separation factor or equilibrium parameter,  $R_L$  (Weber and Chakravorti 1974).

$$R_L = 1/(1 + bC_0), \quad (1)$$

where  $b$  is the Langmuir isotherm constant and  $C_0$  is the initial concentration of fluoride ( $\text{mg L}^{-1}$ ). The  $R_L$ -values between 0 and 1 indicate favorable adsorption for all the temperatures studied. The values of  $R_L$  are given in Table 2.

#### Dubinin–Radushkevich isotherm

The Dubinin–Radushkevich isotherm helps in understanding the type of adsorption from the data of fluoride both in the adsorbent and solution at equilibrium. The linear plot of  $\ln q_e$  vs  $\varepsilon^2$  indicates the applicability of D–R isotherm. The values of  $K_{DR}$ ,  $X_m$  and  $E$  are shown in Table 2. The magnitude of mean free energy of adsorption  $E$  gives information about the type of adsorption mechanism. The  $E$  values are less than  $8 \text{ kJ mol}^{-1}$  which indicate that the fluoride removal was governed by adsorption mechanism (Viswanathan and Meenakshi 2009; Bering et al. 1972).

From the above isotherm analyses, it can be concluded that based on the values of ‘ $r$ ’ the isotherms fit with the fluoride adsorption system in the following order: Freundlich > Langmuir > Dubinin–Radushkevich isotherm.

#### Thermodynamic treatment of the adsorption process

Thermodynamic parameters associated with the adsorption, viz., standard free energy change ( $\Delta G^0$ ), standard enthalpy change ( $\Delta H^0$ ) and standard entropy change ( $\Delta S^0$ ) were calculated as follows. The free energy of adsorption process, considering the adsorption equilibrium coefficient  $K_0$ , is given by the equation

$$\Delta G^0 = -RT \ln K_0, \quad (2)$$

where  $\Delta G^0$  is the standard free energy of adsorption ( $\text{kJ mol}^{-1}$ ),  $T$  is the temperature in Kelvin and  $R$  is the universal gas constant ( $8.314 \text{ J mol}^{-1} \text{ K}^{-1}$ ). The adsorption distribution coefficient  $K_0$  was determined from the slope of the plot  $\ln (q_e/C_e)$  against  $C_e$  at different temperatures and extrapolating to zero  $C_e$  according to the method suggested Khan and Singh (1987).

**Table 1** Isotherms and their linear form and plot

Isotherms	Linear form	Plot
Freundlich	$q_e = k_F C_e^{1/n}$	$\log q_e$ vs $\log C_e$
Langmuir	$q_e = (Q^0 b C_e) / (1 + b C_e)$	$C_e/q_e$ vs $C_e$
Dubinin–Radushkevich	$Q_e = X_m \exp(-k_{DR} \varepsilon^2)$	$\ln q_e$ vs $\varepsilon^2$

**Table 2** Isotherms of fluoride adsorption on AHAC

Isotherms	Parameters	Temperature (K)		
		303	313	323
Freundlich	$1/n$	0.915	0.958	0.970
	$n$	1.093	1.044	1.031
	$K_F$ (mg g <sup>-1</sup> ) (L mg <sup>-1</sup> ) <sup>1/n</sup>	3.626	4.493	5.693
	$r$	0.999	0.999	0.999
Langmuir	$Q^0$ (mg g <sup>-1</sup> )	26.028	52.882	74.239
	$b$ (L g <sup>-1</sup> )	0.162	0.092	0.082
	$R_L$	0.117	0.106	0.104
	$r$	0.996	0.993	0.997
Dubinin–Radushkevich	$K_{DR}$ (mol <sup>2</sup> J <sup>-2</sup> )	9.135E-8	7.790E-8	6.291E-8
	$X_m$ (mg g <sup>-1</sup> )	4.591	5.001	5.410
	$E$ (KJ mol <sup>-1</sup> )	2.340	2.533	2.819
	$r$	0.979	0.982	0.985

**Table 3** Thermodynamic parameters of fluoride adsorption on AHAC

Temperature (K)	$\Delta G^0$ (kJ mol <sup>-1</sup> )	$\Delta H^0$ (kJ mol <sup>-1</sup> )	$\Delta S^0$ (kJ mol <sup>-1</sup> K <sup>-1</sup> )
303	-4.85	25.17	0.10
313	-6.34		
323	-6.83		

The adsorption distribution coefficient may be expressed in terms of  $\Delta H^0$  and  $\Delta S^0$  as a function of temperature:

$$\ln K_0 = (\Delta S^0/R) - (\Delta H^0/RT), \quad (3)$$

where  $\Delta H^0$  is the standard enthalpy change (kJ mol<sup>-1</sup>) and  $\Delta S^0$  is the standard entropy change (kJ mol<sup>-1</sup> K<sup>-1</sup>). The values of  $\Delta H^0$  and  $\Delta S^0$  can be obtained from the slope and intercept of a plot of  $\ln K_0$  against  $1/T$ .

The calculated values of thermodynamic parameters are shown in Table 3. The negative values of  $\Delta G^0$  express the spontaneous nature of fluoride adsorption onto AHAC. The value of  $\Delta H^0$  is positive indicating that the adsorption process is endothermic. The positive value of  $\Delta S^0$  shows the increased randomness at the solid/solution interfaces during fluoride adsorption (Kamaraj et al. 2015c, d).

### Adsorption kinetics

Adsorption kinetic parameters are useful for the prediction of adsorption rate that gives important information for modeling the process and designing adsorption-based water treatment systems (Ganvir and Das 2011; Lakshmi and Vasudevan 2013; Kamaraj et al. 2014a, b). Two adsorption kinetic models, pseudo-first-order and pseudo-second-order models, were studied by using the data obtained from the fluoride adsorption on AHAC at different experimental

conditions. A simple pseudo-first order kinetic model (Lagergren 1898) is given as

$$\log(q_e - q_t) = \log q_e - k_1 t / 2.303, \quad (4)$$

where  $q_t$  is the amount of fluoride on the surface of the AHAC at time  $t$  (mg g<sup>-1</sup>) and  $k_1$  is the equilibrium rate constant of the pseudo-first-order adsorption (min<sup>-1</sup>). The linear plots of  $\log(q_e - q_t)$  against  $t$  give straight lines indicating the applicability of pseudo-first-order model. The slope of the straight line plot of  $\log(q_e - q_t)$  against  $t$  with respect to adsorption at different temperatures viz., 303, 313 and 323 K gives the values of the pseudo-first-order rate constant ( $k_1$ ) and  $r$  which are listed in Table 4.

In addition, the pseudo-second-order model is also widely used and the most popular linear form of pseudo-second-order model is (Ho 2006)

$$t/q_t = 1/h + t/q_e, \quad (5)$$

where  $qt = q_e^2 k_2 t / (1 + q_e k_2 t)$ , the amount of fluoride on the surface of AHAC at any time,  $t$  (mg g<sup>-1</sup>),  $k_2$  is the pseudo-second-order rate constant (g mg<sup>-1</sup> min<sup>-1</sup>),  $q_e$  is the amount of fluoride ion adsorbed at equilibrium (mg g<sup>-1</sup>) and the initial adsorption rate,  $h = k_2 q_e^2$  (mg g<sup>-1</sup> min<sup>-1</sup>). The value of  $q_e$  (1/slope),  $k_2$  (slope<sup>2</sup>/intercept) and  $h$  (1/intercept) of the pseudo-second-order equation can be found out experimentally by plotting  $t/q_t$  against  $t$ . The values of  $q_e$ ,  $k_2$ ,  $h$  and  $r$  of pseudo-second-order model were obtained from the plots of  $t/q_t$  vs.  $t$  for fluoride adsorption at different temperatures viz., 303, 313 and 323 K and are presented in Table 4. The values of  $q_e$  increase with the increase in temperature indicating that the fluoride adsorption increases with rise in temperature. The higher  $r$  values obtained for pseudo-second-order model than pseudo-first-order model show the applicability of pseudo-second-order model. Fluoride adsorption on AHAC

**Table 4** Kinetic parameters of various fluoride concentrations onto AHAC at various temperatures

Kinetic models	Parameters	303 K			313 K			323 K		
		2 mg L <sup>-1</sup>	6 mg L <sup>-1</sup>	10 mg L <sup>-1</sup>	2 mg L <sup>-1</sup>	6 mg L <sup>-1</sup>	10 mg L <sup>-1</sup>	2 mg L <sup>-1</sup>	6 mg L <sup>-1</sup>	10 mg L <sup>-1</sup>
Pseudo-first-order	$k_f$ (min <sup>-1</sup> )	0.075	0.092	0.093	0.094	0.115	0.099	0.091	0.109	0.102
	$r$	0.986	0.991	0.986	0.992	0.980	0.988	0.980	0.980	0.988
	SD	0.115	0.112	0.142	0.106	0.211	0.138	0.106	0.211	0.138
Pseudo-second -order	$q_e$ (mg g <sup>-1</sup> )	1.093	3.213	5.421	1.097	3.251	5.499	1.100	3.288	5.607
	$k_2$ (g mg <sup>-1</sup> min <sup>-1</sup> )	0.069	0.027	0.014	0.079	0.028	0.015	0.089	0.030	0.015
	$h$ (mg g <sup>-1</sup> min <sup>-1</sup> )	0.083	0.276	0.410	0.095	0.299	0.450	0.108	0.322	0.468
Intra particle diffusion	$r$	0.999	0.999	0.999	0.999	0.999	0.999	0.999	0.999	0.999
	SD	0.285	0.290	0.156	0.985	0.308	0.182	1.305	0.340	0.195
	$k_i$ [mg g <sup>-1</sup> (min <sup>0.5</sup> ) <sup>-1</sup> ]	0.092	0.265	0.459	0.090	0.264	0.458	0.087	0.261	0.464
Particle diffusion	$R$	0.977	0.960	0.972	0.963	0.945	0.966	0.961	0.941	0.964
	SD	0.038	0.149	0.212	0.048	0.173	0.234	0.047	0.179	0.242
	$k_p$ (min <sup>-1</sup> )	0.041	0.051	0.115	0.047	0.061	0.116	0.050	0.077	0.093
	$r$	0.998	0.992	0.961	0.984	0.991	0.970	0.971	0.990	0.994
	SD	0.059	0.140	0.692	0.177	0.174	0.610	0.255	0.228	0.215

is a chemisorption process, involving chemical bonding between adsorbent active sites and adsorbate valance forces as suggested by earlier study (Ho and McKay 1999).

These results suggest that experimental data for the adsorption kinetics of fluoride ions on the AHAC better fit the pseudo-second order kinetic model (Ho and McKay 1999). The values of the pseudo-second order rate constant,  $k_2$ , quoted in Table 4, decrease with the increase of the initial fluoride concentration. When the values of correlation coefficients of pseudo-first-order and second-order kinetic models are compared, the  $r$  values for pseudo-second-order kinetic model are higher than that of the values of  $r$  for the pseudo-first-order kinetic model (Table 4). This indicates that the kinetic modeling of the fluoride adsorption onto the AHAC well followed the pseudo-second-order rate model with the correlation coefficients record higher than 0.99 in the present work.

**Diffusion-based models**

For a solid–liquid adsorption process, the solute transfer is usually characterized either by particle diffusion or by intra particle diffusion control. An equation for the particle diffusion controlled adsorption process (Chanda et al. 1983) is given as follows,

$$\ln(1 - C_t/C_e) = -k_p t, \tag{6}$$

where  $k_p$  is the particle rate constant (min<sup>-1</sup>) which is obtained from the slope of the plot between  $\ln(1 - C_t/C_e)$  and  $t$ .

Weber (Weber and Morris 1964) proposed a theory which refers intra particle diffusion model and its equation is

$$q_t = k_i t^{1/2}, \tag{7}$$

where  $k_i$  is the intra-particle rate constant [mg g<sup>-1</sup> (min<sup>0.5</sup>)<sup>-1</sup>]. The slope of the plot of  $q_t$  against  $t^{1/2}$  will give the value of intra-particle rate constant.

The straight line plots of  $\ln(1 - C_t/C_e)$  vs.  $t$  and  $q_t$  vs  $t^{1/2}$  indicate the applicability of particle and intra-particle diffusion models, respectively. The  $k_p$ ,  $k_i$  and  $r$  values at different temperatures viz., 303, 313 and 323 K for both particle and intra-particle diffusion models are given in Table 4. The  $r$  values of both particle and intra particle diffusion models are almost comparable and propose that the fluoride distribution on AHAC follow both the models.

**Fitness of the kinetic models**

The assessment of the employed kinetic models for fitting the adsorption data was made with standard deviation (SD) and the model which possess lower values of SD show better fit to adsorption data. The SD values of AHAC for

**Table 5** Variations of water quality parameters before and after treatment

Water quality parameters	Thoppinayakanpatti		Akkarakaran patti		Silukuvarpatti	
	Before treatment	After treatment	Before treatment	After treatment	Before treatment	After treatment
F <sup>-</sup> (mg L <sup>-1</sup> )	3.14	0.17	3.32	0.19	3.30	0.15
pH	8.12	7.92	7.66	7.89	7.11	7.41
EC (ms)	1558	1.414	3397	3184	2789	1983
TDS (mg L <sup>-1</sup> )	1013	919	2373	1948	1952	1289
Salinity (mg L <sup>-1</sup> )	1424	1244	1843	1728	1504	1443
Na <sup>+</sup> (mg L <sup>-1</sup> )	146.1	128.1	251.2	178.7	230.2	154.8
K <sup>+</sup> (mg L <sup>-1</sup> )	9.6	7.2	8.29	7.45	10.36	8.14
TH (mg L <sup>-1</sup> )	152.8	114.4	189.8	127.9	94.2	67.8

all the kinetic models are summarized in Table 4. Smaller SD values were observed for the pseudo-second-order and intra-particle diffusion models which indicate that these two models are significant in the fluoride adsorption process and suggest that the adsorption of fluoride ion onto the pores of AHAC.

### Field study

The fluoride adsorption capacity of AHAC was tested using ground water samples collected from three different villages of Nilakottai block viz., Thoppinayakan patti, Akkarakarn patti and Silukuvarpatti. Ground water samples of these villages are highly contaminated with fluoride. About 0.1 g of the sorbent was added to 100 ml of ground water sample and was shaken well for constant time interval and at room temperature. The data obtained for fluoride and other physicochemical parameters before and after treatment are given in Table 5. It is evident from the results that the AHAC can be effectively employed for removing the fluoride from water.

### Comparative evaluation of chemically modified biomass based adsorbents

Comparisons of various chemically modified biomass based adsorbents are given in Table 6. The AHAC used in this study showed adsorption capacity of fluoride 26.03 mg g<sup>-1</sup>, which was higher than chemically modified bio-sorbents such Zirconium impregnated cashew nut shell carbon (Alagumuthu and Rajan 2010), Pecan nut shell carbon modified with eggshell carbon (Hernandez-Montoya et al. 2012), Pine wood bio-char (Mohan et al. 2012), aluminum hydroxide coated pumice (Salifu et al. 2013), Scandinavia spruce wood modified with aluminium and iron oxides (Tchomgui-Kamga et al. 2010), KMnO<sub>4</sub> modified activated carbon from steam pyrolysis of rice straw (Daifullah et al. 2007), ammonium carbonate activated carbon of *Tamarindus indica* fruit shell (Sivasankar et al. 2012), activated bagasse carbon of sugarcane (Yadav et al. 2013), polypyrrole grafted peanut shell carbon (Li et al. 2016), Pine sawdust modified with AlCl<sub>3</sub>-Binary system (Vazquez-Guerrero et al. 2016) and K<sub>2</sub>CO<sub>3</sub> activated

**Table 6** Comparison of the fluoride adsorption capacities of different chemically modified adsorbents

Adsorbent	pH	Adsorption capacity (mg g <sup>-1</sup> )	References
Ammonium carbonate activated carbon of <i>Tamarindus indica</i> fruit shell	7.1	22.33	Sivasankar et al. (2012)
Zirconium impregnated cashew net ( <i>Anacardium occidentale</i> ) shell carbon	7.0	2.32	Alagumuthu and Rajan (2010)
Pecan ( <i>Carya illinoensis</i> ) nut shell carbon modified with eggshells carbon	7.0	2.51	Hernandez-Montoya et al. (2012)
Pine wood bio-char	2.0	9.77	Mohan et al. (2012)
Scandinavian spruce wood modified with aluminium and iron oxides	6.9	13.64	Tchomgui-Kamga et al. (2010)
KMnO <sub>4</sub> modified activated carbon from steam pyrolysis of rice straw	2.0	15.9	Daifullah et al. (2007)
Aluminum hydroxide coated pumice	7.0	11.90	Salifu et al. (2013)
Activated bagasse carbon of sugarcane	6.0	1.15	Yadav et al. (2013)
Polypyrrole grafted peanut shell carbon	8.0	17.15	Li et al. (2016)
Pine sawdust modified with AlCl <sub>3</sub> -binary system	7.0	9.16	Vazquez-Guerrero et al. (2016)
K <sub>2</sub> CO <sub>3</sub> activated cotton nut shells	7.0	2.47	Mariappan et al. (2015)
Aluminium hydroxide coated activated carbon from bark of <i>Morinda tinctoria</i>	7.0	26.03	Current study

cotton nut shells (Mariappan et al. 2015). Experiments were initially conducted to evaluate the effect of fluoride adsorption capacity of prepared activated carbon alone, the results were showed very minimum adsorption capacity was  $3.48 \text{ mg g}^{-1}$ . After coating of activated carbon with aluminum hydroxide, the fluoride removal capacity were tremendously increased up to  $26.03 \text{ mg g}^{-1}$ , this is attributed due to the increase amount of aluminum hydroxide on activated carbon. As a result, the entire study was carried out with AHAC. The performance of AHAC was better when compared to other adsorbents. As the adsorption capacity of AHAC for fluoride removal is maximum in neutral pH, it is suitable for field level application, since no pH adjustment is required.

## Conclusion

The present study concludes that bark of *M. tinctoria* can be effectively used as a raw material for the preparation of aluminum hydroxide coated activated carbon by chemical modification. Prepared AHAC was found to be a promising material for the removal of fluoride from aqueous solution even at domestic level. Adsorption capacity was found to be maximum at neutral pH, which is one of the merits of the adsorbent used. Freundlich isotherm and intra-particle diffusion were the best-fitting models for the adsorption of fluoride on AHAC. The  $\Delta H^0$  value was positive in the temperature range of 303, 313 and 323 K. This indicates that the adsorption process was endothermic. The negative  $\Delta G^0$  values at different temperatures indicate the spontaneous nature of the sorption of fluoride onto the AHAC. The positive  $\Delta S^0$  value suggests good affinity of fluoride ions towards AHAC. The rate of reaction follows pseudo-second-order kinetics. Adsorption process follows chemisorption.

**Acknowledgments** The first author (AA) is grateful to the UGC for the fellowship under Research Fellowship in Sciences for Meritorious Students. The authors also thank the authorities of GRI for the encouragement.

**Open Access** This article is distributed under the terms of the Creative Commons Attribution 4.0 International License (<http://creativecommons.org/licenses/by/4.0/>), which permits unrestricted use, distribution, and reproduction in any medium, provided you give appropriate credit to the original author(s) and the source, provide a link to the Creative Commons license, and indicate if changes were made.

## References

- Alagumuthu G, Rajan M (2010) Equilibrium and kinetics of adsorption of fluoride onto zirconium impregnated cashew nut shell carbon. *Chem Eng J* 158:451–457
- Amalraj A, Pius A (2013) Health risk from fluoride exposure of a population in selected areas of Tamil Nadu South India. *Food Sci Hum Wellness* 2:75–86
- Amalraj A, Pius A (2014) Removal of selected basic dyes using activated carbon from tannery wastes. *Sep Sci Technol* 49:90–100
- APHA (2005) Standard methods for examination of water and wastewater, 21st edn. American Public Health Association, Washington, DC
- Ayoob S, Gupta AK (2006) Fluoride in drinking water: a review on the status and stress effects. *Crit Rev Environ Sci Technol* 36:433–487
- Ba Y, Huang H, Yang Y, Cui L, Zhu J, Zhu C, Liu J, Zhang Y (2009) The association between osteocalcin gene polymorphism and dental fluorosis among children exposed to fluoride in People's Republic of China. *Ecotoxicol Environ Saf* 72:2158–2161
- Bering BP, Dubinin MM, Serpenski VV (1972) On thermodynamics of adsorption on micropores. *J Colloid Interface Sci* 38:185–194
- Bhatnagar M, Bhatnagar A, Jha S (2002) Interactive biosorption by microalgal biomass as a tool for fluoride removal. *Biotechnol Lett* 24:1079–1081
- Chanda M, O'Driscoll KF, Rempel GL (1983) Sorption of phenolics onto cross-linked poly (4-vinyl pyridine). *React Polym* 1:281–293
- Chen N, Zhang Z, Feng C, Zhu D, Yang Y, Sugiura N (2011) Preparation and characterization of porous granular ceramic dispersed aluminum and iron oxides as adsorbent for fluoride removal from aqueous solution. *J Hazard Mater* 186:863–868
- Daifullah AAM, Yakout SM, Elreefy SA (2007) Adsorption of fluoride in aqueous solutions using  $\text{KMnO}_4$ -modified activated carbon derived from steam pyrolysis of rice straw. *J Hazard Mater* 147:633–643
- Das DP, Das J, Parida K (2003) Physicochemical characterization and adsorption behaviour of calcined Zn/Al hydrotalcite-like compound towards removal of fluoride from aqueous solution. *J Colloid Interface Sci* 261:213–220
- Das N, Pattanaik P, Das R (2005) Defluoridation of drinking water using activated titanium rich bauxite. *J Colloid Interface Sci* 292:1–10
- Eskandarpour A, Onyango MS, Ochieng A, Asai S (2008) Removal of fluoride ions from aqueous solution at low pH using schwertmannite. *J Hazard Mater* 152:571–579
- Fawell J, Bailey K, Chilton J, Dahi E, Fewtrell L, Magara Y (2006) Fluoride in drinking water. IWA Publishing, London
- Freundlich HMF (1906) Über die adsorption in lösungen. *Z Phys Chem* 57A:385–470
- Ganvir V, Das K (2011) Removal of fluoride from drinking water using aluminum hydroxide coated rice husk ash. *J Hazard Mater* 185:1287–1294
- Hernandez-Montoya V, Ramirez-Montoya LA, Bonilla-Petriciolet A, Montes-Moran MA (2012) Optimizing the removal of fluoride from water using new carbons obtained by modification of nut shell with a calcium solution from egg shell. *Biochem Eng J* 62:1–7
- Ho YS (2006) Second order kinetic model for the sorption of cadmium on to tree fern: a comparison of linear and non linear methods. *Water Res* 40:119–125
- Ho YS, McKay G (1999) Pseudo-second order model for sorption processes. *Process Biochem* 34:451–465
- Jacks G, Rajagopalan K, Alveteg T, Jonsson M (1993) Genesis of high-F groundwaters, Southern India. *Appl Geochem* 2:241–244
- Kamaraj R, Davidson DJ, Sozhan G, Vasudevan S (2014a) An in situ electrosynthesis of metal hydroxides and their application for adsorption of 4-chloro-2-methylphenoxyacetic acid (MCPA) from aqueous solution. *J Environ Chem Eng* 2:2068–2077

- Kamaraj R, Davidson DJ, Sozhan G, Vasudevan S (2014b) Adsorption of 2, 4-dichlorophenoxyacetic acid (2, 4-D) from water by in situ generated metal hydroxides using sacrificial anodes. *J Taiwan Inst Chem Eng* 45:2943–2949
- Kamaraj R, Vasudevan S (2015a) Decontamination of selenate from aqueous solution by oxidized multi-walled carbon nanotubes. *Powder Technol* 274:268–275
- Kamaraj R, Vasudevan S (2015b) Evaluation of electrocoagulation process for the removal of strontium and cesium from aqueous solution. *Chem Eng Res Des* 93:522–530
- Kamaraj R, Davidson DJ, Sozhan G, Vasudevan S (2015c) Adsorption of herbicide 2-(2, 4-dichlorophenoxy)propanoic acid by electrochemically generated aluminum hydroxides: an alternative to chemical dosing. *RSC Adv* 5:39799–39809
- Kamaraj R, Ganesan P, Vasudevan S (2015d) Removal of lead from aqueous solutions by electrocoagulation: isotherm, kinetics and thermodynamic studies. *Int J Environ Sci Technol* 12:683–692
- Khaled A, El-Nemr A, El-Sikily A, Abdelwahab O (2009) Removal of direct blue 106 from artificial textile dye effluent using activated carbon from orange peel; adsorption isotherm and kinetic studies. *J Hazard Mater* 165:100–110
- Khan AA, Singh RP (1987) Adsorption thermodynamics of carbafuran on Sn (IV) arsenosilicate in  $H^+$ ,  $Na^+$  and  $Ca^{2+}$  forms. *Colloids Surf* 24:33–42
- Kruse E, Ainchil J (2003) Fluoride variations in groundwater of an area in Buenos Aires province. *Argent Environ Geol* 44:86–89
- Kumar E, Bhatnagar A, Ji M, Jung W, Lee SH, Kim SJ, Lee G, Song H, Choi JY, Yang JS, Jeon BH (2009) Defluoridation from aqueous solutions by granular ferric hydroxide (GFH). *Water Res* 43:490–498
- Lagergren S (1898) Zur theorie der sogenannten adsorption gelöster stoffe. *Kungliga Svenska Vetenskapsakademiens. Handlingar* 24:1–39
- Lakshmi J, Vasudevan S (2013) Graphene—a promising material for removal of perchlorate ( $ClO_4^-$ ) from water. *Environ Sci Pollut Res* 20:5114–5124
- Langmuir I (1916) The constitution and fundamental properties of solids and liquids. *J Am Chem Soc* 38:2221–2295
- Legroui A, Badreddine M, Barroug A, Roy AD, Besse JP (1999) Influence of pH on the synthesis of the Zn–Al–nitrate layered double hydroxide and the exchange of nitrate by phosphate ions. *J Mater Sci Lett* 18:1077–1079
- Lesmana SO, Febriana N, Soetaredjo FE, Sunarso J, Ismadji S (2009) Studies on potential applications of biomass for the separation of heavy metals from water and wastewater. *Biochem Eng J* 44:19–41
- Li Y, Liang CK, Katz PB, Niu S, Cao S, Stookey GK (1996) Effect of fluoride exposure and nutrition on skeletal fluorosis. *J Dent Res* 75:2699
- Li C, Chen N, Zhao Y, Li R, Feng C (2016) Polypyrrole-grafted peanut shell biological carbon as a potential sorbent for fluoride removal: sorption capability and mechanism. *Chemosphere* 163:81–89
- Lua AC, Yang T (2004) Effects of vacuum pyrolysis conditions on the characteristics of activated carbons derived from pistachio-nut shells. *J Colloid Interface Sci* 276:364–372
- Ma Y, Wang S, Fan M, Gong W, Gao B (2009) Characteristics and defluoridation performance of granular activated carbons coated with manganese oxides. *J Hazard Mater* 168:1140–1146
- Maliyekkal SM, Shukla S, Philip L, Nambi IM (2008) Enhanced fluoride removal from drinking water by magnesia-amended activated alumina granules. *Chem Eng J* 140:183–192
- Mandinic Z, Curcic M, Antonijevic B, Carevic M, Mandic J, Djukic-Cosic D, Lekic CP (2010) Fluoride in drinking water and dental fluorosis. *Sci Total Environ* 408:3507–3512
- Mariappan R, Vairamuthu R, Ganapathy A (2015) Use of chemically activated cotton nut shells carbon for the removal of fluoride contaminated drinking water: kinetics evaluation. *Chin J Chem Eng* 23:710–721
- Meenakshi, Maheshwari RC (2006) Fluoride in drinking water and its removal. *J Hazard Mater B* 137:456–463
- Meenakshi S, Pius A, Karthikeyan G, Appa Rao BV (1991) The pH dependent of efficiency of activated alumina in defluoridation of water. *Indian J Environ Prot* 11:511–513
- Mohan D, Sharma R, Singh VK, Steele P, Pittman CU (2012) Fluoride removal from water using bio-char, a green waste, low-cost adsorbent: equilibrium uptake and sorption dynamics modeling. *Ind Eng Chem Res* 51:900–914
- Onyango MS, Kojima Y, Aoyi O, Bernardo EC, Matsuda H (2004) Adsorption equilibrium modeling and solution chemistry dependence of fluoride removal from water by trivalent-cation-exchanged zeolite. *J Colloid Interface Sci* 279:341–350
- Orion Star and Star Plus Meter User Guide (2008) Thermo Fisher Scientific Inc
- Raichur AM, Basu MJ (2001) Adsorption of fluoride onto mixed rare earth oxides. *Sep Purif Technol* 24:121–127
- Salame II, Bandosz TJ (2000) Comparison of the surface features of two wood-based activated carbons. *Ind Eng Chem Res* 39:301–306
- Salifu A, Petrusovski B, Ghebremichael K, Modestus L, Buamah R, Aubry C, Amy GL (2013) Aluminum (hydr)oxide coated pumice for fluoride removal from drinking water: synthesis, equilibrium, kinetics and mechanism. *Chem Eng J* 228:63–74
- Sathish RS, Raju NSR, Raju GS, Rao GN, Kumar KA, Janardhana C (2007) Equilibrium and kinetic studies for fluoride adsorption from water on zirconium impregnated coconut shell carbon. *Sep Sci Technol* 42:769–788
- Shorter JP, Massawe J, Parry N, Walker RW (2010) Comparison of two village primary schools in northern Tanzania affected by fluorosis. *Int Health* 2:269–274
- Sivasankar V, Rajkumar S, Muruges S, Darchen A (2012) Influence of shaking or stirring dynamic methods in the defluoridation behavior of activated tamarind fruit shell carbon. *Chem Eng J* 197:162–172
- Susheela AK, Majumdar K (1998) Guide on water and excreta related diseases for grassroot level functionaries IEC 04, Rajiv Gandhi National Drinking Water Mission and National Institute of Rural Development, Govt. of India
- Tchomgui-Kamga E, Alonzo V, Nansou-Njiki CP, Audebrand N, Ngameni E, Darchen A (2010) Preparation and characterization of charcoals that contain dispersed aluminum oxide as adsorbents for removal of fluoride from drinking water. *Carbon* 48:333–343
- Vasudevan S, Oturan MA (2014) Electrochemistry: as cause and cure in water pollution—an overview. *Environ Chem Lett* 12:97–108
- Vasudevan S, Lakshmi J, Sozhan G (2009) Studies on a Mg–Al–Zn alloy as an anode for the removal of fluoride from drinking water in an electrocoagulation process. *Clean* 37:372–378
- Vasudevan S, Suresh Kannan B, Lakshmi J, Mohanraj S, Sozhan G (2011) Effects of alternating and direct current in electrocoagulation process on the removal of fluoride from water. *J Chem Technol Biotechnol* 86:428–436
- Vazquez-Guerrero A, Alfaro-Cuevas-Villanueva R, Rutiaga-Quinones JG, Cortés-Martínez R (2016) Fluoride removal by aluminum-modified pine sawdust: effect of competitive ions. *Ecol Eng* 94:365–379
- Viswanathan N, Meenakshi S (2009) Synthesis of Zr(IV) entrapped chitosan polymeric matrix for selective fluoride sorption. *Colloids Surf B* 72:88–93



- Waidyasekera PGK, Nikaido T, Weerasinghe DDS, Wettasinghe KA, Tagami J (2007) Caries susceptibility of human fluorosed enamel and dentine. *J Dent* 35:343–349
- Weber TW, Chakravorti RK (1974) Pore and solid diffusion models for fixed bed adsorbers. *J Am Inst Chem Eng* 20:228–238
- Weber WJ, Morris JC (1964) Equilibria and capacities for adsorption on carbon. *J Sanit Eng Div* 90:79–91
- WHO (2006) Chemical fact sheets: fluoride, guidelines for drinking water quality (electronic resource), vol 1. 3rd edn incorporation. First Addendum, Recommendations, Geneva, pp 375–377
- WHO (2008) Guidelines for drinking water quality incorporating 1st and 2nd addenda, recommendations, 3rd edn. World Health Organization, Geneva
- Xiong X, Liu J, He W, Xia T, He P, Chen X, Yang K, Wang A (2007) Dose–effect relationship between drinking water fluoride levels and damage to liver and kidney functions in children. *Environ Res* 103:112–116
- Yadav AK, Abbassi R, Gupta A, Dadashzadeh M (2013) Removal of fluoride from aqueous solution and groundwater by wheat straw, sawdust and activated bagasse carbon of sugarcane. *Ecol Eng* 52:211–218
- Yang J, Qiu K (2010) Preparation of activated carbons from walnut shells via vacuum chemical activation and their application for methylene blue removal. *Chem Eng J* 165:209–217